Title	New Efficient and Accurate Method of Nonlinear Analysis of Offshore Tubular Frames (the Idealized Structural Unit Method) (Report I) : Development of Static Theory and Method(Mechanics, Strength & Structure Design)
Author(s)	Ueda, Yukio; Rashed, Sherif M. H.; Nakacho, Keiji
Citation	Transactions of JWRI. 1999, 28(1), p. 67-77
Version Type	VoR
URL	https://doi.org/10.18910/9763
rights	
Note	

New Efficient and Accurate Method of Nonlinear Analysis of Offshore Tubular Frames (the Idealized Structural Unit Method) (Report I)†

— Development of Static Theory and Method —

Yukio UEDA*, Sherif M. H. RASHED** and Keiji NAKACHO***

Abstract

The Idealized Structural Unit Method[1), 2)] is applied to the analysis of nonlinear behavior of three-dimensional offshore tubular frames. For this purpose a "tubular structural unit" is developed and used to analyze the entire behavior of the frame until final collapse. In this method, large deflections, instability, plasticity and the effect of residual stresses and initial out-of-straightness are considered. Modeling of a structure is very simple since large structural units are regarded as elements. The required computer effort is very small although achieving a high degree of accuracy and reliability. In this report, the theory and method are developed for static problems.

KEY WORDS : (Offshore Structure) (Tubular Frame) (Ultimate Strength) (Nonlinear Behavior) (Plasticity) (Buckling) (Idealized Structural Unit) (Super Finite Element)

1. Introduction

Despite the vast development in the area of nonlinear structural analysis, there is still an urgent need of accurate, reliable and efficient tools for the analysis of nonlinear behavior of steel tubular offshore structures until collapse. In the analysis, geometric and material nonlinearities of the structure must be incorporated. Inevitable loss of stiffness of structural components before and after the state of ultimate strength have been reached must be taken into account.

An elastic analysis, linear or nonlinear, is insufficient to consider post ultimate strength behavior of structural members.

The finite element method can analyze the behavior of tubular frames to the required degree of accuracy with consideration of geometric and material nonlinearities. This method, however, could be very expensive when analyzing a large-sized structure.

To overcome this difficulty many brace models have been proposed. Zayas, et al.[1)] have classified these models into two groups. The first is the "physical theory brace models" presented by Higginbotham[2)], Nilforoushan[3)] and Singh[4)]. They used a pin-ended model with equivalent effective length and a plastic hinge at the center. The analytical formulations are based on assuming an axial force-moment interaction curve and an elastic-perfect plastic moment-curvature relationship at the center hinge. The second group is the "phenomenological brace models". The basis of these models is to pre-define the shape of the axial force-axial displacement response of a truss element representing the brace by employing either mathematical or empirical results. Models of this type have been developed by Higginbotham[2)], Nilforoushan[3)], Singh[4)], Marshall[5)], Roeder[6)], Jain[7)] and Maison[8)]. In these models, however, only the axial force acting on the member is considered. End moments and/or lateral load are not taken into account. These, in many cases, have a large effect on buckling and post-buckling behavior of braces.

Ueda and Rashed[9), 10)] have suggested the idealized structural unit method (ISUM) for the analysis of nonlinear behavior of large sized redundant structures. The method has been successfully applied to ship structures[9), 10), 11), 12)]. In this method the structure is divided into the biggest possi-

† Received on July 30, 1999
* Professor Emeritus (Professor, Kinki University)
** MSC Japan Ltd.
*** Associate Professor

Transactions of JWRI is published by Joining and Welding Research Institute of Osaka University, Ibaraki, Osaka 567-0047, Japan.

ble "structural units" (equivalent to an element in the conventional finite element method), such as a part of a girder between two vertical web stiffeners or a stiffened panel bounded by 4 primary supporting members. Geometric and material nonlinear behavior of the components of a structural unit, such as buckling of plate elements, collapse of flanges or stiffeners, etc. are idealized and described in concise forms related to forces and displacements of a limited number of nodal points at the boundaries of the structural unit. These concise forms are a set of failure interaction surfaces and a set of stiffness matrices expressing the behavior of the unit before and after these failures. The load is applied incrementally and the response of the structure is analyzed. The required computer effort is very small. The accuracy and reliability of the method are maintained in comparison with the finite element method.

In this study the method is extended to analyze the nonlinear behavior of three-dimensional offshore tubular structures. For this purpose a "tubular structural unit" is developed and applied to offshore steel tubular structures. In this report, the theory and method are developed for the static problem where the load is applied to the structure statically.

2. The Tubular Structural Unit

Offshore tubular space frames are usually constructed of several tubular chords (legs) braced by a large number of tubular bracing members. A member running between two joints is usually a prismatic circular tube. The thickness of the members is increased locally at the joints to increase their strength. In the analysis, the structure may be modeled as a group of prismatic members connected at the joints. Each member is referred to as the "tubular structural unit."

The tubular structural unit is represented in **Fig. 1**. It is a prismatic circular tube with each end connected to a joint. The equilibrium and compatibility conditions at each end are expressed with respect to a nodal point that is located on the central line of the tube.

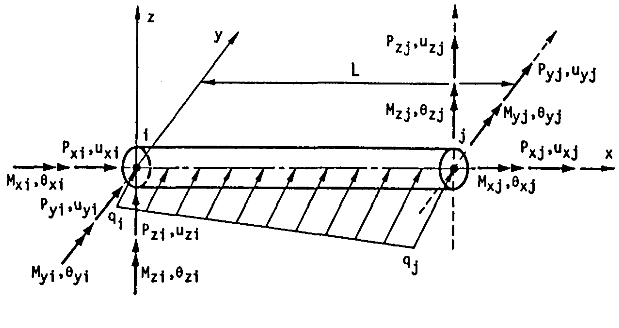

Fig. 1 The tubular structural unit

Six degrees of freedom are considered at each nodal point as shown in Fig. 1. Nodal displacement and nodal force vectors U and R may be expressed, respectively, as follows:

$$U = \begin{Bmatrix} U_i \\ U_j \end{Bmatrix}, \quad R = \begin{Bmatrix} R_i \\ R_j \end{Bmatrix} \tag{1}$$

where

$$U_i = \{u_{xi} \quad u_{yi} \quad u_{zi} \quad \theta_{xi} \quad \theta_{yi} \quad \theta_{zi}\}^T$$
$$U_j = \{u_{xj} \quad u_{yj} \quad u_{zj} \quad \theta_{xj} \quad \theta_{yj} \quad \theta_{zj}\}^T$$
$$R_i = \{P_{xi} \quad P_{yi} \quad P_{zi} \quad M_{xi} \quad M_{yi} \quad M_{zi}\}^T$$
$$R_j = \{P_{xj} \quad P_{yj} \quad P_{zj} \quad M_{xj} \quad M_{yj} \quad M_{zj}\}^T$$

$\{\ \}^T$: transposed matrix of $\{\ \}$

In this method, the effect of laterally distributed loads acting on the member is fully considered in the solution of the equilibrium differential equation in order to detect their local phenomena as described in the following sections.

A tubular structural unit is dealt as a beam column. Highly nonlinear behavior of beam columns has been studied by many researchers. D. R. Sherman, et al., have studied the behavior of tubular members subjected to bending[13] and combined bending and axial load[14]. W. F. Chen and D. A. Ross[15] have studied the behavior of fabricated tubular members with consideration of residual stresses and out-of-straightness. D. J. Han and W. F. Chen[16] have investigated post-buckling and cyclic behavior of tubular members. Many other works may be found in the literature. Based on these studies, an outline of the behavior of the tubular structural unit is described as basic information for idealization.

When the unit is subjected to an increasing load, various types of failures may take place depending on the dimensions and material of the unit, its boundary conditions and the ratio of the load components. If the diameter-thickness ratio of a tube is larger than about 70[17], local buckling of the tube shell may take place where high compressive stresses exist. For highly compressed members this ratio is usually much lower than 70. This failure mode is then not considered in this study.

When tubes of lower diameter-thickness ratios and high or medium slenderness ratios are subjected to a load combination with a dominating axial compression, they show overall elastic or elastic-plastic buckling followed by plastic collapse. Plastic collapse occurs when plastic hinges are formed at the regions of maximum bending moment (mid-span and fixed or restrained ends) so that a collapse mechanism is formed. When the bending moments and/or the distributed lateral loads are pronounced, the tube tends to deflect laterally until plastic collapse takes place as before. Tubes subjected to load combinations having axial tensile loads do not buckle, and only plastic collapse is expected.

Tubes with very low slenderness ratios do not buckle and they show only plastic collapse, irrespective of the ratio of the load components.

After the formation of the first plastic hinge at the region of maximum bending moment, the internal forces cannot be increased any more at the plastic zone. However, the tube may continue to deform. The ratio of the internal force components acting at the plastic zone may also change depending on the nature of the overall structure and the external loads acting on it. Other plastic hinges may be formed at other regions of the tube, if the internal force components at these regions become sufficient.

The behavior of the structural unit, before and after failure, may be expressed by the relationship of the nodal forces R to the nodal displacements U. Since the behavior is nonlinear, the incremental method is applied in this study.

3. Failure-Free Stiffness Matrix

Before buckling or yielding takes place, the behavior of the structural unit considered as a beam column may be expressed by the following differential equation:

$$\begin{aligned} \frac{d^4 w_y}{dx^4} + k^2 \frac{d^2 w_y}{dx^2} &= \frac{1}{EI} q_y \\ \frac{d^4 w_z}{dx^4} + k^2 \frac{d^2 w_z}{dx^2} &= \frac{1}{EI} q_z \end{aligned} \tag{2}$$

where

w_y and w_z = lateral deflections in the xy and zx planes

$k = \sqrt{P/EI}$ is a common variable in the two equations

P = internal axial force

E = Young's modulus

I = cross-sectional moment of inertia

q_y and q_z = components of the lateral load q in y and z directions. For a linearly distributed load

$$q_m = q_{mi}\{1 + (\alpha - 1)x/L\}$$

$$\alpha = q_{mj}/q_{mi}, \quad m = y, z$$

These two equations may be solved independently. When the internal axial force P is compressive (positive), the general solution of the first of equations (2) may be written as

$$w_y = a\cos kx + b\sin kx + cx + d + f(q_y) \tag{3}$$

$f(q_y)$ is dependent on the distribution of the lateral load q_y. The constants of integration a, b, c and d are determined from the following boundary conditions (see **Fig.2**):

$$x = 0 \qquad w_y = u_{yi}, \quad dw_y/dx = \theta_{zi}$$

$$x = L \qquad w_y = u_{yj}, \quad dw_y/dx = \theta_{zj}$$

The bending moment M_z may be expressed as

$$M_z = -EI\, d^2 w_y / dx^2 \tag{4}$$

Using equation (4), M_{zi} and M_{zj} may be expressed in terms of nodal displacements as in Appendix I. Applying the equilibrium condition, nodal force components P_{yi} and P_{yj} may be found and expressed as in Appendix I. Similarly M_{yi}, M_{yj}, P_{zi} and P_{zj} may be derived from the second of equations (2).

The relationship between the nodal axial forces P_{xi} and P_{xj}, and the nodal axial displacements u_{xi} and u_{xj} may be expressed as

$$P_{xi} = -P_{xj} = EA(u_{xi} - u_{xj} - u_b)/L \tag{5}$$

where

u_b = axial shortening due to bending of the structural unit, which is obtained by the following equation:

$$\begin{aligned} u_b &= \int_0^L (ds - dx) \\ &= \frac{1}{2}\int_0^L \left\{ (dw_y/dx)^2 + (dw_z/dx)^2 \right\} dx \end{aligned} \tag{6}$$

Introducing the expressions for w_y and w_z into equation (6) and performing the integration, u_b may be obtained and expressed as in Appendix I.

The relationship between the twisting moments M_{xi} and M_{xj}, and the rotations θ_{xi} and θ_{xj} may be expressed with the usual one for a beam.

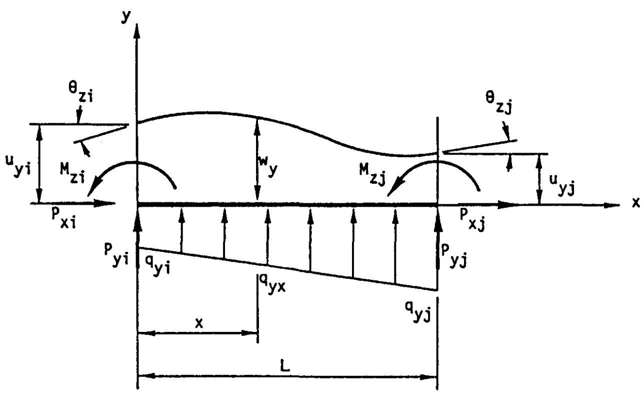

Fig. 2 Projection of the structural unit on the xy plane

Neglecting small terms of higher order, as increment of the nodal force ΔR may be expressed as follows :

$$\Delta R + \Delta Q = K \Delta U \tag{7}$$

where

K = tangential stiffness matrix

ΔQ = load vector associated with the distributed load applied on the unit.

K and ΔQ are given in Appendix I.

When the internal axial force is tensile (negative), the same K and ΔQ are obtained in which

$$a_1 = (\sinh k^*L - k^*L) \Big/ \left\{ k^*(1 - \cosh k^*L) \right\}$$
$$a_2 = 2 + (k^*L \sinh k^*L) \big/ (1 - \cosh k^*L)$$
$$k^* = \sqrt{|P|/EI}$$

It should be noticed that the effect of the lateral load appears not only in the vector ΔQ but also in the tangential stiffness matrix K.

4. Ultimate Strength of Tubular Members

The nodal force-displacement relationship, equation (7) holds until the structural unit buckles or yielding starts. After yielding has started even locally, the stiffness of the structural unit decreases, however, equation (7) is assumed to hold in the analysis until the unit buckles or one or more full plastic cross sections are developed.

In the following, the conditions of the buckling strength and the full plastic strength of a cross section are represented and the ultimate strength condition is constructed as the combination of these.

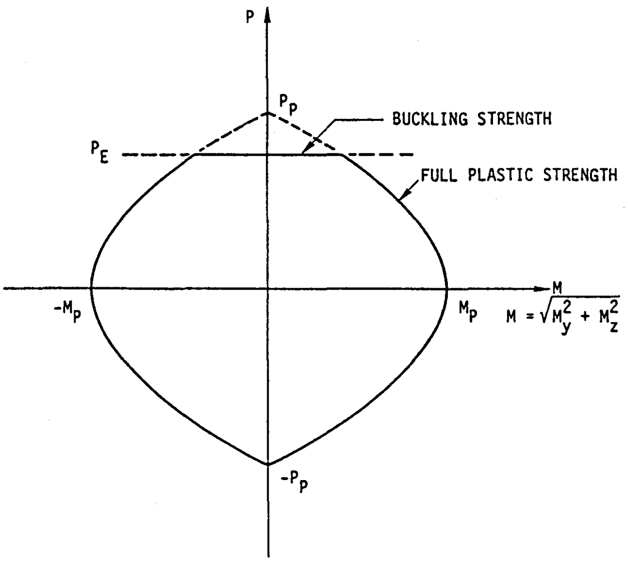

Fig. 3 Ultimate strength interaction relationship

4.1 Buckling strength

Chen and Atsuta[18] reported a summary of extensive studies done in Lehigh University[19]. Three columns curves have been produced for different cross sections, methods of manufacturing and steel grades. These curves are adopted in this study. Short columns do not buckle and they may attain their full plastic axial compressive strength. In this case the magnitude of P_B reaches that of P_P.

4.2 Effective length for buckling

The effective length L_{eij} of a structural unit ij rigidly connected at nodal points i and j to other structural units in the plane of buckling (in case of plane frames) is given in reference[20]. L_{eij} is estimated by comparing bending stiffnesses of member ij and restraining members.

In a space frame, however, restraining members do not generally lie in the plane of rotation due to buckling. A restraining member normal to that plane contributes with its torsional rigidity. The restraining stiffness of any member depends on its relative orientation. The structural unit ij may then buckle in the manner which has minimum total restraint at the ends i and j. Buckling is generally accompanied with some twist of the structural unit, since the planes of minimum restraint at i and j are generally different.

The determination of the planes of minimum restraint and the buckling configuration is a complicated and time-consuming process. However, the restraining stiffness at nodal points i and j about y and z axes may be obtained from the global tangential stiffness matrix and the restraining stiffnesses at i and j may be determined.

4.3 Full plastic strength

In this analysis, the effect of shearing stresses on plastic strength is assumed to be negligible. Then the internal shearing forces P_y and P_z, and the internal twisting moment M_x do not affect the full plastic strength interaction relationship.

Integrating the full plastic axial stress over the cross sectional area, expressions for the axial force P_x and bending moments M_y and M_z may be obtained. These expressions may be combined to obtain the full plastic strength function

$$\Gamma_P = \frac{\left|\sqrt{M_y^2 + M_z^2}\right|}{M_P} - \cos\left(\frac{\pi |P|}{2P_P}\right) = 0 \tag{8}$$

where

M_P and P_P = magnitudes of the full plastic bending moment and the full plastic axial force of the cross section

Equation (8) may be represented as shown in **Fig 3**.

4.4 Ultimate strength interaction relationship

Depending on the properties of the structural unit and the nature of the increasing load vector applied on it, it reaches the buckling strength, or the plastic strength. The assembly of these conditions represents the ultimate strength interaction relationship of the tubular structural unit as shown in Fig.3.

5. Ultimate Strength Stiffness Matrix

As the load increases, the ultimate strength condition, may be satisfied at nodal point i, nodal point j and/or the location of maximum bending moment along the unit. The internal force vector at such a location cannot further increase. However, the unit may continue to deform while redistribution of the internal forces takes place, and the ratio of the components of the internal force vector may change. In the following, the stiffness matrix of such a structural unit is derived:

(a) First, let a structural unit in which equation (8) is satisfied at nodal point i and /or j be considered. A plastic node[21] is inserted at the nodal point(s) where equation (8) is satisfied. Equation (8) is regarded as a plastic potential and plastic flow theory is applied. An increment of nodal displacement vector, ΔU, is composed to the elastic component ΔU^e and the plastic component ΔU^p; that is,

$$\Delta U = \Delta U^e + \Delta U^p \tag{9}$$

Based on the plastic flow theory, ΔU^p is expressed as follows:

$$\Delta U^p = \begin{Bmatrix} \Delta U_i^p \\ \Delta U_j^p \end{Bmatrix} = \begin{bmatrix} \lambda_i & 0 \\ 0 & \lambda_j \end{bmatrix} \begin{Bmatrix} (\partial \Gamma_p / \partial R)_i \\ (\partial \Gamma_p / \partial R)_j \end{Bmatrix} = \lambda \, \phi \tag{10}$$

where

λ_i and λ_j = positive scalars.

In the process of analysis, if the sign of λ_i or/and λ_j is detected negative, unloading occurs at the plastic node and the node should de dealt as an elastic one.

The incremental stiffness equation may be written as follows:

$$\Delta R + \Delta Q = K \Delta U^e = K(\Delta U - \Delta U^p) \tag{11}$$

ΔR satisfies the condition of plasticity that $\Delta \Gamma_p$ should be equal to zero.

$$\Delta \Gamma_p = \phi^T \Delta R = 0 \tag{12}$$

Equations (11) and (12) give the relationship between λ and ΔU. Substituting this relation into equation (11), equation (11) may be written as

$$\Delta R + \Delta Q^p = K^p \Delta U \tag{13}$$

where

ΔQ^p = elastic-plastic incremental force vector of the distributed load

K^p = elastic-plastic stiffness matrix

(b) If equation (8) is satisfied at point a, the position of maximum bending moment along the length of the unit, the unit is divided at this position into two beam-column elements ia and aj. A plastic node is inserted at point a on either element ia or element aj. Considering the condition of nodal points i and j, elastic or elastic-plastic stiffness matrices and distributed load vectors are evaluated for the two elements. Then the extra nodal displacements at point a are eliminated in the normal way.

(c) If the magnitude of the axial compressive force reaches that of buckling, the structural unit buckles and is allowed to deflect until equation (8) is satisfied at any point along its length, where a plastic node is then inserted as in (b).

In (b) and (c), the position of maximum bending moment is usually very close to the mid-length of the unit. In the analysis it may be reasonably assumed at the mid-length.

6. Idealization of Behavior and Assessment of Its Accuracy

When a tubular structural unit is subjected to an increasing load, the internal force vectors at the nodes and the mid-length of the structural unit may take any of the paths expressed in **Fig.4**. These may be idealized as shown in the same figure.

In the analysis, the nonlinear behavior of the unit is idealized so that the unit deforms elastically, as expressed by the stiffness equation, equation (7), until the ultimate strength condition is satisfied at node i, node j or/and the mid-length. The behavior of the unit is then expressed by the ultimate strength stiffness matrix derived in the previous section.

Figure 5 presents examples of comparison among test results of 18 tubular members subjected to axial compression and end bending moments[22], those of elastic plastic large deformation finite element analyses and those obtained using the tubular structural unit. In the finite element analyses a member is divided into 8 beam-column elements with large deflection and plastic capabilities. Each element has 40 integration points along the circumference of the member at the middle of the element. It may be seen that the unit is capable of accurate representation of the behavior of tubular members. Of particular practical interest, loss of stiffness prior to ultimate strength and post-buckling loss of strength are accurately predicated.

In this method the elastic stiffness matrix is derived based on equation (2) in which the differentiation is with respect to the distance x along the original axis. This causes an error in calculating the axial force when the elastic deflection becomes very large. However this error is very small (about 1.5 percent for a central deflection of 0.11 of the length between points of zero bending moment). Such large deflections are not expected before buckling of the member. After buckling, the member is divided into two elements whose coordinates are updated at each load step. No sensible error is expected for tubes practically used in offshore structures for the whole post-buckling range. It is to be noted however, that local buckling of the tube wall is not taken into account. Tubes with high D/t ratio may need an investigation of their rotation capacity if the analysis is to be performed very far beyond buckling of the tubes. Cracking due to lack of ductility is also not taken into account.

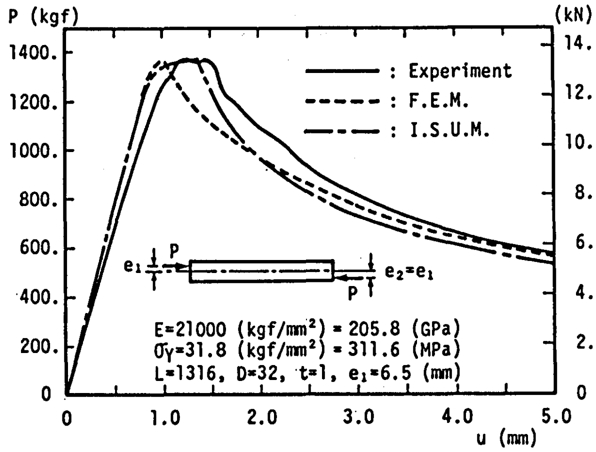

(a) A case of collapse after buckling

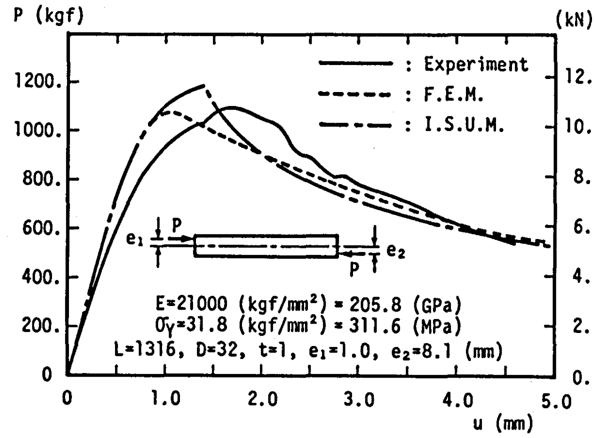

(b) A case of collapse due to bending

Fig. 5 Comparisons of load-shortening curves of tubular members

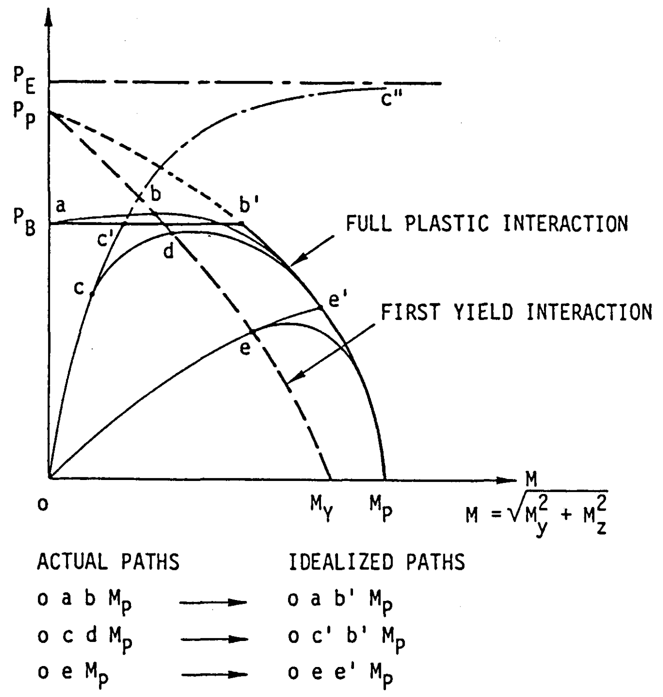

Fig. 4 Idealization of tubular structural units

7. Procedure of Analysis and Numerical Example

When a structure consisting of a group of tubular members is subjected to an increasing load, the internal forces in the members increase until one member or more show local failure. However, redistribution of internal forces may take place in the structural members and further load may be supported. The structure reaches its ultimate strength when successful redistribution of internal forces cannot be achieved and equilibrium can not be attained without reduction of load. The structure may continue to deform while the external load decreases, and/or increases again depending on the nature of the structure and the applied load.

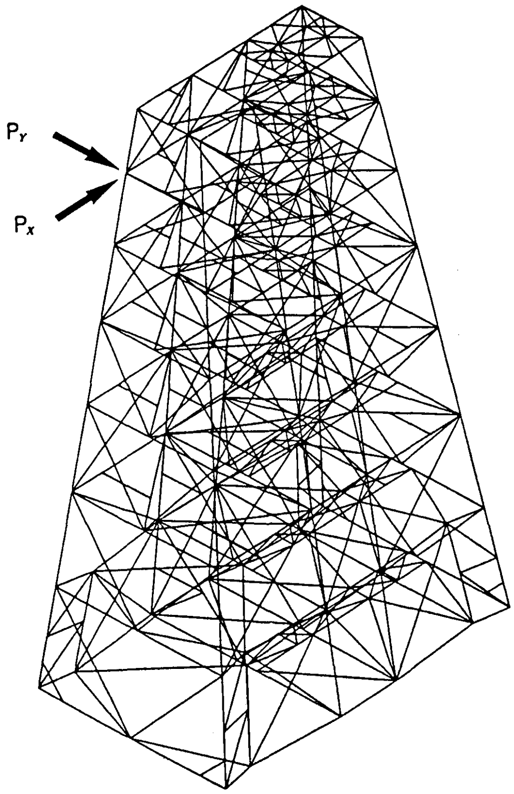

Fig. 6 A jacket structure and applied collision load

For the analysis, a structure is divided into the above developed tubular structural units and the incremental load method is used. First, the load-free structure is considered. The incremental stiffness matrix of each structural unit is constructed and transformed into the global coordinates. The global incremental stiffness matrix of the whole structure is then assembled. After the boundary conditions are introduced the first load increment is applied. The deformation of the structure is obtained and the internal forces in each structural unit are evaluated. Each structural unit is then checked for bucking and/or plasticization.

Since the stiffness matrix of the tubular structural unit is dependent on deformation and internal forces, a new stiffness matrix is constructed and transformed into global coordinates for each structural unit after each load increment. The global stiffness matrix is reassembled and the next increment of loads is applied.

When buckling and/or plasticization of one structural unit or more are detected within a loading step, the load increment is scaled down to that just necessary to cause such failure. This prevents the internal force vectors from shooting out of the ultimate strength interaction surfaces.

The ultimate strength of the structure is detected by consideration of plastic deformation.

Following the procedure outlined in the foregoing, a computer program, NOAMAS, has been completed and used to analyze several structures. **Figure 6** presents one of these structures. It is a jacket being 117.6 m in height standing in a 114.0 m depth of water.

The jacket supports a total deck load of 16,000 tons. A collision situation is simulated by applying a horizontal load at level -4.600 m as shown in the figure. The relation between the collision load and the displacement of the point of colliding is presented in **Fig. 7**. The area under the curves represents the absorbed energy. The numbers in the figure show the sequence and locations of plasticizations. The analysis was terminated when the energy of the colliding ship has been absorbed by the structure. Eight members have shown local failures during the course of collision, however the global structure did not collapse.

The model has 303 nodal points and 771 structural units. Deck load has been applied in one step and the collision load in 30 steps. Intermediate iterations are carried out to ensure proper plastic deformation. The analysis consumed 135 s on a CRAY-1 computer.

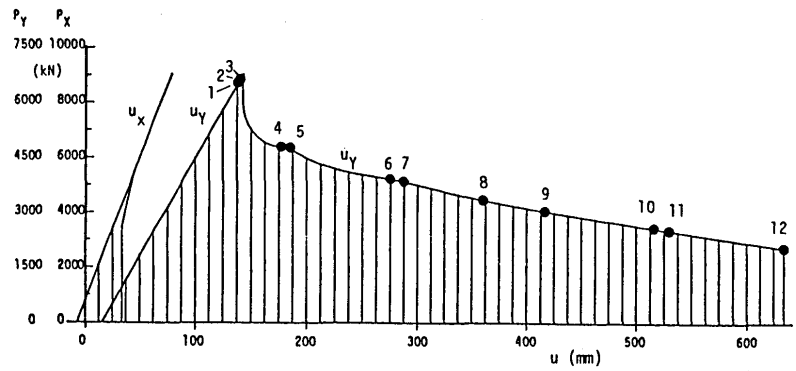

(a) Load-displacement relationship at point of collision

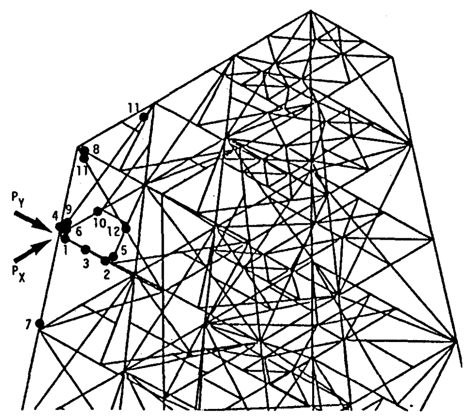

(b) Sequence and locations of plasticizations

Fig. 7 Results of ultimate strength analysis of a jacket

8. Summary and Conclusions

In this paper the idealized structural unit method (ISUM) is applied to the analysis of nonlinear behavior of offshore tubular space frames until final collapse. For this purpose the tubular structural unit is developed. The behavior of tubular members described by the tubular structural unit is compared with the results of experiments and those of a refined analysis by the finite element method. Very good agreement has been observed, especially with respect to loss of stiffness before the ultimate strength has been reached, as well as the ultimate strength and the subsequent loss of strength.

A computer program, NOAMAS, has been completed and an example of analysis of a jacket structure is presented.

In this analysis, modeling of a structure is very simple and the required computer effort is very small, although giving high accuracy and reliability. With these advantages, this method is proven to be an efficient and accurate method of analysis of nonlinear behavior of large-sized offshore tubular space frames, with several applications to nonlinear design problems. For example, the ultimate limit state of a tubular frame in different loading situations, the energy absorbed by sub-global and global deformation in a major collision situation, may be accurately and economically evaluated.

References

1) Y. Ueda and S. M. H. Rashed : An Ultimate Transverse Strength Analysis of Ship Structure, Journal of the Society of Naval Architects of Japan, Vol. 136 (1974), pp.309-324 (in Japanese).
2) Y. Ueda and S. M. H. Rashed : The Idealized Structural Unit Method and Its Application to Deep Girder Structures, Computer and Structures, Vol.18 (1984), pp.277-293.
3) V. A. Zayas, et al. : Inelastic Structural Analysis of Braced Platforms for Seismic Loading, OTC3979 (1981).
4) A. B. Higginbotham : The Inelastic Cyclic Behavior of Axially-Loaded Steel Members, Dissertation (1973), University of Michigan.
5) R. Nilforoushan : Seismic Behavior of Multi-story K-braced Frame Structures, University of Michigan Research Report UMEE73R9 (1973).
6) P. Singh : Seismic Behavior of Braces and Braced Steel Frame," Dissertation (1977), University of Michigan.
7) P. W. Marshall : Design Considerations for Offshore Structures Having Nonlinear Response to Earthquakes, Preprint (1978), ASCE Annual Convention and Exposition (Chicago).
8) C. W. Roeder and E. P. Popov : Inelastic Behavior of Eccentricity Braced Frames Under Cyclic Loading, EERC Report No. 77-18 (1977), Earthquake Engineering Research Center, University of California.
9) A. K. Jain and S. C. Goel : Hysteresis Models for Steel Members Subjected to Cyclic Buckling or Cyclic End Moments and Buckling, University of Michigan Research Report UMEE78R6 (1978).
10) B. Maison and E. P. Popov : Cyclic Response Prediction for Braced Steel Frame, Journal of the Structural Division (July 1980), ASCE.
11) Y. Ueda, S. M. H. Rashed and M. Katayama : Ultimate Strength Analysis of Double Bottom Structures by Idealized Structural Unit Method, Journal of the Society of Navel Architects of Japan, Vol. 138 (1975), pp.322-329 (in Japanese).
12) Y. Ueda, et al. : Ultimate Strength of the Double Bottom Standing on a Rock, Journal of the Society of Navel Architects of Japan, Vol. 143 (1978), pp.334-345 (in Japanese).
13) D. R. Sherman : Tests of Circular Tubes in Bending, Journal of the Structural Division (Nov. 1976), ASCE.
14) D. R. Sherman, H. Erzurumlu and W. Mueller : Behavioral Study of Circular Tubular Beam-Columns, Journal of the Structural Division (June 1974), ASCE.
15) W. F. Chen and D. A. Ross : Tests of Fabricated Tubular Columns, Journal of the Structural Division (Mar. 1977), ASCE.
16) D. J. Han and W. F. Chen : Buckling and Cyclic Inelastic Analysis of Steel Tubular Beam-Columns, Engineering Structures, Vol. 5 (1983).
17) J. G. Bouwkamp : Buckling and Post-Buckling Strength of Circular Tubular Sections, Offshore Technology Conference (1975), Paper No. OTC2204.
18) W. F. Chen and T. Atsuta : Theory of Beam-Columns, Vol. 1 (1976), McGraw-Hill Inc..
19) R. Bjorhovde : Deterministic and Probabilistic Approaches to the Strength of Steel Columns, Ph.D. Dissertation in Civil Engineering (1972), Lehigh University.
20) A. Selberg : Steel Structures, Tapir (1972), Norway (in Norwegian).
21) Y. Ueda, et al. : A New Theory on Elastic-Plastic Analysis of Framed Structures, Technology Reports of the Osaka University, Vol. 19 (1969), No. 875.
22) H. Kjeoy and G. Foss ; Tests on Buckling Strength and Post Buckling Behavior of Cylindrical Members Subjected to End Moments and Axial Compressive Load, Veritas Report No. 80-0625 (1980), Det Norske Veritas.
23) Y. Ueda and T. Yao : The Plastic Node Method - A New Method of Plastic Analysis, Computer Methods in Applied Mechanics and Engineering, Vol. 34 (1982), Nos. 1-3, pp.1089-1104.

APPENDIX I

Expressions for Nodal Moments, Shearing Forces and Shortening due to Bending

1. Nodal Moments

$$M_{zi} + M_{zqi} = \frac{P}{a_2}(u_{yi} - u_{yj}) + P\frac{a_1 + L}{a_2}\theta_{zi} - P\frac{a_1}{a_2}\theta_{zj}$$

$$M_{zj} + M_{zqj} = \frac{P}{a_2}(u_{yi} - u_{yj}) - P\frac{a_1}{a_2}\theta_{zi} + P\frac{a_1 + L}{a_2}\theta_{zj}$$

$$M_{zqi} = q_{yi}\left\{\frac{1}{2k^2}\left(2 - k^2 L\frac{a_1 + 2L/3}{a_2}\right) - \frac{\alpha L}{2}\frac{a_1 + L/3}{a_2}\right\}$$

$$M_{zqj} = q_{yi}\left\{\frac{L}{2}\frac{a_1 + L/3}{a_2} - \frac{\alpha}{2k^2}\left(2 - k^2 L\frac{a_1 + 2L/3}{a_2}\right)\right\}$$

2. Nodal Shearing Forces

$$P_{yi} + P_{yqi} = -P_{yj} - P_{yqj} = \frac{P(2-a_2)}{a_2 L}(u_{yi} - u_{yj}) + \frac{P}{a_2}(\theta_{zi} + \theta_{zj})$$

$$P_{yqi} = q_{yi}\left\{\frac{L}{3} + \frac{\alpha L}{6} + \frac{(1-\alpha)}{2k^2 L}\left(2 - \frac{k^2 L^2}{3a_2}\right)\right\}$$

$$P_{yqj} = q_{yi}\left\{\frac{\alpha L}{3} + \frac{L}{6} + \frac{(\alpha-1)}{2k^2 L}\left(2 - \frac{k^2 L^2}{3a_2}\right)\right\}$$

3. Shortening due to Bending

$$\begin{aligned} u_b = L\Big[& d_1\left\{(\theta_{yi} + \theta_{yj} + 2\phi_z)^2 + (\theta_{zi} + \theta_{zj} + 2\phi_y)^2\right\} + d_2\left\{(\theta_{yi} - \theta_{yj})^2 + (\theta_{zi} - \theta_{zj})^2\right\} + (\phi_z^2 + \phi_y^2)/2 \\ & + d_3\left\{q_{zi}(\theta_{yi} + \theta_{yj} + 2\phi_z) + q_{yi}(\theta_{zi} + \theta_{zj} + 2\phi_y)\right\} + d_4\left\{q_{zi}(\theta_{yi} - \theta_{yj}) + q_{yi}(\theta_{zi} - \theta_{zj})\right\} \\ & + d_5(q_{zi}\phi_z + q_{yi}\phi_y) + d_6(q_{zi}^2 + q_{yi}^2)\ \Big] \end{aligned}$$

$$d_1 = \frac{k^2L^2 + kL\sin kL - 4(1-\cos kL)}{16\left(kL\cos\frac{kL}{2} - 2\sin\frac{kL}{2}\right)^2}$$

$$d_2 = -a_1/(8L)$$

$$d_3 = \frac{1}{2}\left\{(\alpha-1)\left(\frac{L}{k^2L^2P} - \frac{kL\sin kL}{2(1-\cos kL) - kL\sin kL}\frac{L}{12P}\right) - d_5\right\}$$

$$d_4 = \frac{1}{2}\left(\frac{L}{2P}\frac{\sin kL}{kL(1-\cos kL)} - \frac{1}{k^2LP}\right)(1+\alpha) + d_2\frac{(1+\alpha)L}{P}$$

$$d_5 = \frac{L}{12P}(\alpha - 1)$$

$$d_6 = \frac{L^2}{P^2}\left(\frac{3\sin kL + kL}{8kL(1-\cos kL)} - \frac{1}{k^2L^2} + \frac{1}{24}\right)$$

$$\phi_z = (u_{zi} - u_{zj})/L, \qquad \phi_y = (u_{yi} - u_{yj})/L, \qquad \alpha = q_{yj}/q_{yi} = q_{zj}/q_{zi}$$

4. Tangential Stiffness Matrix and Distributed Load

$$K = \eta_0 \begin{bmatrix} 1 & \gamma_{1y} & \gamma_{1z} & 0 & -\gamma_{2z} & \gamma_{2y} & -1 & -\gamma_{1y} & -\gamma_{1z} & 0 & -\gamma_{3z} & \gamma_{3y} \\ & \eta_1 + \gamma_{1y}^2 & \gamma_{1y}\gamma_{1z} & 0 & -\gamma_{1y}\gamma_{2z} & \eta_3 + \gamma_{1y}\gamma_{2y} & -\gamma_{1y} & -\eta_1 - \gamma_{1y}^2 & -\gamma_{1y}\gamma_{1z} & 0 & -\gamma_{1y}\gamma_{3z} & \eta_3 + \gamma_{1y}\gamma_{3y} \\ & & \eta_1 + \gamma_{1z}^2 & 0 & -\eta_3 - \gamma_{1z}\gamma_{2z} & \gamma_{1z}\gamma_{2y} & -\gamma_{1z} & -\gamma_{1z}\gamma_{1y} & -\eta_1 - \gamma_{1z}^2 & 0 & -\eta_3 - \gamma_{1z}\gamma_{3z} & \gamma_{1z}\gamma_{3y} \\ & & & \eta_5 & 0 & 0 & 0 & 0 & 0 & -\eta_5 & 0 & 0 \\ & & & & \eta_2 + \gamma_{2z}^2 & -\gamma_{2z}\gamma_{2y} & \gamma_{2z} & \gamma_{2z}\gamma_{1y} & \eta_3 - \gamma_{2z}\gamma_{1z} & 0 & \eta_4 + \gamma_{2z}\gamma_{3z} & -\gamma_{2z}\gamma_{3y} \\ & & & & & \eta_2 + \gamma_{2y}^2 & -\gamma_{2y} & -\eta_3 - \gamma_{2y}\gamma_{1y} & \gamma_{2y}\gamma_{1z} & 0 & -\gamma_{2y}\gamma_{3z} & \eta_4 + \gamma_{2y}\gamma_{3y} \\ & & & & & & 1 & \gamma_{1y} & \gamma_{1z} & 0 & \gamma_{3z} & -\gamma_{3y} \\ & & & & & & & \eta_1 + \gamma_{1y}^2 & \gamma_{1y}\gamma_{1z} & 0 & \gamma_{1y}\gamma_{3z} & -\eta_3 - \gamma_{1y}\gamma_{3y} \\ & & \text{SYM.} & & & & & & \eta_1 + \gamma_{1z}^2 & 0 & \eta_3 + \gamma_{1z}\gamma_{3z} & -\gamma_{1z}\gamma_{3y} \\ & & & & & & & & & \eta_5 & 0 & 0 \\ & & & & & & & & & & \eta_2 + \gamma_{3z}^2 & -\gamma_{3z}\gamma_{3y} \\ & & & & & & & & & & & \eta_2 + \gamma_{3y}^2 \end{bmatrix}$$

$$\Delta Q = \begin{Bmatrix} \Delta q_{yi} g_y + \Delta q_{zi} g_z \\ \Delta q_{yi}(f_1 + \gamma_{1y} g_y^*) \\ \Delta q_{zi}(f_1 + \gamma_{1z} g_z^*) \\ 0 \\ -\Delta q_{zi}(f_2 + \gamma_{2z} g_z^*) \\ \Delta q_{yi}(f_2 + \gamma_{2y} g_y^*) \\ -\Delta q_{yi} g_y - \Delta q_{zi} g_z \\ \Delta q_{yi}(f_3 + \gamma_{1y} g_y^*) \\ \Delta q_{zi}(f_3 + \gamma_{1z} g_z^*) \\ 0 \\ -\Delta q_{zi}(f_4 + \gamma_{3z} g_z^*) \\ \Delta q_{yi}(f_4 + \gamma_{3y} g_y^*) \end{Bmatrix},$$

$$\eta_0 = EA/(Le)$$
$$\eta_1 = P(2 - a_2)/(a_2 L \eta_0)$$
$$\eta_2 = P(a_1 + L)/(a_2 \eta_0)$$
$$\eta_3 = P/(a_2 \eta_0)$$
$$\eta_4 = -P a_1/(a_2 \eta_0)$$
$$\eta_5 = GJ/(L\eta_0)$$
$$a_1 = (\sin kL - kL)/(1 - \cos kL)$$
$$a_2 = -2\{(kL \sin kL)/(1 - \cos kL)\}$$

$$\gamma_{1n} = \frac{d\eta_1\eta_0}{dP} L\phi_n + \frac{d\eta_3\eta_0}{dP}(\theta_{mi} + \theta_{mj}) - q_{ni}\frac{df_1}{dP}$$

$$\gamma_{2n} = \frac{d\eta_3\eta_0}{dP} L\phi_n + \frac{d\eta_2\eta_0}{dP}\theta_{mi} + \frac{d\eta_4\eta_0}{dP}\theta_{mj} - q_{ni}\frac{df_2}{dP}$$

$$\gamma_{3n} = \frac{d\eta_3\eta_0}{dP} L\phi_n + \frac{d\eta_2\eta_0}{dP}\theta_{mj} + \frac{d\eta_4\eta_0}{dP}\theta_{mi} - q_{ni}\frac{df_4}{dP}$$

$$f_1 = \frac{L}{3} + \frac{\alpha L}{6} + (1-\alpha)\frac{1}{2k^2L}\left(2 - \frac{k^2L^2}{3a_2}\right)$$

$$f_2 = \frac{1}{2k^2}\left(2 - k^2L\frac{a_1 + 2L/3}{a_2}\right) - \frac{\alpha L}{2}\frac{a_1 + L/3}{a_2}$$

$$f_3 = \frac{\alpha L}{3} + \frac{L}{6} + (\alpha - 1)\frac{1}{2k^2L}\left(2 - \frac{k^2L^2}{3a_2}\right)$$

$$f_4 = \frac{L}{2}\frac{a_1 + L/3}{a_2} - \frac{\alpha}{2k^2}\left(2 - k^2L\frac{a_1 + 2L/3}{a_2}\right)$$

$$g_n = \left\{d_3(\theta_{mi} + \theta_{mj} + 2\phi_n) + d_4(\theta_{mi} - \theta_{mj}) + d_5\phi_n + 2d_6 q_{ni}\right\}/e$$

$$g_n^* = \left(\Delta q_{yi} g_y + \Delta q_{zi} g_z\right)/\Delta q_{ni}$$

$$e = \left\{1 + EA(b_{y1} + b_{z1})\right\}$$

$$b_{n1} = \frac{dd_1}{dP}(\theta_{mi} + \theta_{mj} + 2\phi_n)^2 + \frac{dd_2}{dP}(\theta_{mi} - \theta_{mj})^2 + \frac{dd_3}{dP} q_{ni}(\theta_{mi} + \theta_{mj} + 2\phi_n)$$
$$+ \frac{dd_4}{dP} q_{ni}(\theta_{mi} - \theta_{mj}) + \frac{dd_5}{dP} q_{ni}\phi_n + \frac{dd_6}{dP} q_{ni}^2$$

$$\phi_n = (u_{ni} - u_{nj})/L$$

$$m = y, z, \quad n = z, y$$

APPENDIX II

Explicit Forms of the Elastic-Plastic Stiffness Matrix and Incremental Distributed Load Vector

(a) End i Plastic and End j Elastic

$$K^P = \begin{bmatrix} K_{ii} - K_{ii}\phi_i\phi_i^T K_{ii}/A_1 & K_{ij} - K_{ii}\phi_i\phi_i^T K_{ij}/A_1 \\ K_{ji} - K_{ji}\phi_i\phi_i^T K_{ii}/A_1 & K_{jj} - K_{ji}\phi_i\phi_i^T K_{ij}/A_1 \end{bmatrix}, \qquad \Delta Q^P = \begin{Bmatrix} \Delta Q_i - (B_1/A_1)K_{ii}\phi_i \\ \Delta Q_j - (B_1/A_1)K_{ji}\phi_i \end{Bmatrix}$$

$$A_1 = \phi_i^T K_{ii}\phi_i, \qquad B_1 = \phi_i^T \Delta Q_i$$

(b) End i Elastic and End j Plastic

$$K^p = \begin{bmatrix} K_{ii} - K_{ij}\phi_j\phi_j^T K_{ji}/A_2 & K_{ij} - K_{ij}\phi_j\phi_j^T K_{jj}/A_2 \\ K_{ji} - K_{jj}\phi_j\phi_j^T K_{ji}/A_2 & K_{jj} - K_{jj}\phi_j\phi_j^T K_{jj}/A_2 \end{bmatrix}, \qquad \Delta Q^p = \begin{Bmatrix} \Delta Q_i - (B_2/A_2)K_{ij}\phi_j \\ \Delta Q_j - (B_2/A_2)K_{jj}\phi_j \end{Bmatrix}$$

$$A_2 = \phi_j^T K_{jj}\phi_j \ , \qquad B_2 = \phi_j^T \Delta Q_j$$

(c) Both Sides Plastic

$$K^p = \begin{bmatrix} K_{ii} & K_{ij} \\ K_{ji} & K_{jj} \end{bmatrix} - \frac{1}{A}\begin{bmatrix} K_{ii}\phi_i & K_{ij}\phi_j \\ K_{ji}\phi_i & K_{jj}\phi_j \end{bmatrix}\begin{bmatrix} A_2\phi_i^T K_{ii} - A_{12}\phi_j^T K_{ji} & A_2\phi_i^T K_{ij} - A_{12}\phi_j^T K_{jj} \\ A_1\phi_j^T K_{ji} - A_{21}\phi_i^T K_{ii} & A_1\phi_j^T K_{jj} - A_{21}\phi_i^T K_{ij} \end{bmatrix}$$

$$\Delta Q^p = \begin{Bmatrix} \Delta Q_i - \dfrac{1}{A}\left\{(A_2B_1 - A_{12}B_2)K_{ii}\phi_i + (A_1B_2 - A_{21}B_1)K_{ij}\phi_j\right\} \\ \Delta Q_j - \dfrac{1}{A}\left\{(A_2B_1 - A_{12}B_2)K_{ji}\phi_i + (A_1B_2 - A_{21}B_1)K_{jj}\phi_j\right\} \end{Bmatrix}$$

$$A_{12} = \phi_i^T K_{ij}\phi_j \ , \qquad A_{21} = \phi_j^T K_{ji}\phi_i \ , \qquad A = A_1A_2 - A_{12}A_{21}$$